





Transient Evaluation of Non-Markovian Models by Stochastic State Classes and Simulation

Gabriel Dengler¹ , Laura Carnevali² ,
Carlos E. Budde³ , and Enrico Vicario² 

¹ Saarland University, Saarbrücken, Germany
dengler@depend.uni-saarland.de

² Department of Information Engineering, University of Florence, Florence, Italy

³ DISI, University of Trento, Trento, Italy



Abstract. Non-Markovian models have great expressive power, at the cost of complex analysis of the stochastic process. The method of Stochastic State Classes (SSCs) derives closed-form analytical expressions for the joint Probability Density Functions (PDFs) of the active timers with marginal expolynomial PDF, though being hindered by the number of concurrent non-exponential timers and of discrete events between regenerations. Simulation is an alternative capable of handling the large class of PDFs samplable via inverse transform, which however suffers from rare events. We combine these approaches to analyze time-bounded transient properties of non-Markovian models. We enumerate SSCs near the root of the state-space tree and then rely on simulation to reach the target, affording transient evaluation of models for which the method of SSCs is not viable while reducing computational time and variance of the estimator of transient probabilities with respect to simulation. Promising results are observed in the estimation of rare event probabilities.

1 Introduction

Quantitative evaluation of stochastic timed models is a difficult problem. While the Markovian case counts with time-tested analytical and numerical solutions [5, 6,27,50], non-Markovian models are much harder to analyze [23,24].

Motivation. Our main research goal is to *quantify time-bounded transient properties of non-Markovian systems*. Specifically, non-Markovian models with multiple concurrent timers having non-Exponential general (GEN) distributions [57] capture characteristics of a large variety of systems, such as real-time systems, cyber-physical systems, and software subject to aging. Notably, they have been used to define quantitative safety and liveness properties of safety-critical systems—e.g. in aerospace, railway, and nuclear industries [8,20,38,52]—and to give semantics to RAMS standards—reliability, availability, maintainability, and safety [45,49]—including fault tree analysis and reliability block diagrams [13,48].

The expressive power of non-Markovian models comes at the cost of complex analysis of the underlying stochastic process to evaluate the properties of interest. A relevant example in RAMS engineering is the evaluation of the *system*

reliability, i.e., the probability p to observe an undesired event during mission time, which is a time-bounded safety property φ to check on the model [20,45]. Numerical algorithms such as Value Iteration (VI) can approximate this quantity for Markovian systems [5,17,21], via exhaustive explorations of the states of the model [21,28]. For GEN transitions, VI needs approximations such as phase-type distributions [44,60]. However, besides approximation errors, this exacerbates the state-space explosion problem, which hinders numeric algorithms like VI and ultimately renders them unfit to study non-Markovian models [21,29].

Related Work. Analytical quantification of properties in non-Markovian models is viable only under restrictions on the class of GEN distributions, and on the number of concurrent timers in the stochastic process states [19]. For models subtending a Markov Regenerative Process (MRP) [34], most approaches address the subclass where up to one GEN timer is enabled in each state, i.e. the *enabling restriction* [3,18,26]. The method of supplementary variables [25,55] does not require this restriction theoretically, but is impractical without it [55]. In contrast, sampling the stochastic process at equidistant time points can overcome the enabling restriction [40,61], but requires timers to follow a deterministic (DET) or exponential (EXP) distribution. The compositional approach of [14] does not restrict the number of GEN timers either but requires the underlying stochastic process to be decomposable into a hierarchy of Semi-Markov Processes (SMPs).

Also, the method of Stochastic State Classes (SSCs) [1,31,57] can address models with multiple concurrent GEN timers, provided that a regeneration is always reached in a bounded number of discrete events (the *bounded regeneration restriction*). SSCs are restricted to GEN timers in the expolynomial class—sum of products of EXP and polynomials—which includes EXP, uniform, triangular, and Erlang distributions. The approach derives the closed-form expression of the Probability Density Function (PDF) of the active timers after each discrete event and its applicability is hindered by large numbers of concurrent GEN timers and of discrete events between regenerations.

Simulation can also quantify a (transient) property φ on non-Markovian systems [59]. When formal system models such as Stochastic Time Petri Nets (STPNs) are available, this is called Statistical Model Checking (SMC) [35]. SMC can study any stochastic system whose stochastic kernel is known, and from which samples can be drawn, e.g. via the inverse transform method [2,35,62]. In contrast to analytical methods like SSC analysis, which provide an exact value for the quantity p characterized by φ , sequential SMC generates simulation traces to produce an *estimate* $\langle \hat{p}, \varepsilon \rangle$ s.t. $\hat{p} \in p \pm \varepsilon$ with some desired probability δ . However, this is hindered by *rare events*: when the property φ to be quantified requires simulation traces to visit states that occur with very low probability, then ε or the number of traces explodes, rendering standard simulation useless [53,62].

Rare Event Simulation (RES) tackles such problems, where Importance Splitting (ISPLIT) has been used in SMC to quantify rare transient properties of non-Markovian systems [10,36]. ISPLIT splits the state space $\mathcal{S} = \uplus_{i=0}^n \mathcal{S}_i$ to estimate the conditional probabilities p_i of reaching a state in \mathcal{S}_i from \mathcal{S}_{i-1} , where the states satisfying φ are in \mathcal{S}_n and $p = \prod_{i=1}^n p_i$ [36]. This works when all the

estimates \hat{p}_i can be approached via crude Monte Carlo (MC), which rules out rare events caused by single transitions of very low probability, e.g. EXPs with a very low rate. Such cases can be tackled by Importance Sampling (IS), which changes the PDFs f of concurrent timers for a proposed \tilde{f} , making it more likely to observe states that satisfy φ [37]. An unbiased estimate \hat{p} is then obtained by multiplying the result of MC by the *likelihood ratio* f/\tilde{f} . The drawback of IS is that \tilde{f} is problem-dependent, usually defined ad hoc, and bad choices result in worse-than-MC convergence [37]. Automatic \tilde{f} selection is restricted to specific distributions (mainly EXP) and model structures [12,51], and even adaptive IS approaches such as cross-entropy require non-trivial parameter tuning [9].

Contributions. In this paper, we evaluate time-bounded transient properties of non-Markovian systems by combining state-space analysis via SSCs with simulation, capturing rare events while not incurring state-space explosion [21,57]. To the best of our knowledge, this solution has never been attempted in formal SMC frameworks [4]. To approach it, we enumerate SSCs near the root of the state-space tree and then perform simulation from there on, deriving Confidence Intervals (CIs) for the probability that a property φ of interest is satisfied. Experimental results show that the approach enables evaluation for models for which the method of SSCs is not viable, notably reducing computational time and variance of the probability estimator with respect to both MC simulation and IS. Moreover, promising results are obtained in the estimation of rare event probabilities, opening the way to further research directions.

In the rest of the paper, first we recall background concepts (Sec. 2). Then, we present our approach (Sec. 3) and derive CIs for properties of interest (Sec. 4). Finally, we present experimental results (Sec. 5) and draw conclusions (Sec. 6). Additional experimental and implementation details are in Appendices A and B.

2 Background

In this section, we recall STPNs (Sec. 2.1) as well as aspects of the method of SSCs (Sec. 2.2) and MC simulation (Sec. 2.3) that are relevant for our work.

2.1 Stochastic Time Petri Nets

STPNs [46,57] model concurrent systems with stochastic durations and discrete probabilistic choices. As shown in Fig. 1, an STPN consists of: places with tokens (circles with dots), modeling the discrete logical state; transitions (bars) modeling activities with stochastic duration; directed arcs (directed arrows), from input places to transitions and from transitions to output places, modeling precedence relations among activities. A transition is enabled by a marking (i.e., an assignment of tokens to places) if each of its input places contains at least one token, and its enabling function (“? expression”) evaluates to true.

Upon enabling, a transition samples a time-to-fire from its Cumulative Distribution Function (CDF), i.e., EXP, GEN, or the generalized CDF of a Dirac delta function, where transitions with zero time-to-fire are called immediate (IMM)

(in Fig. 1, IMM and GEN transitions are drawn as thin and thick vertical bars, respectively). The transition with minimum time-to-fire fires, removing one token from each of its input places, adding one token to each of its output places, and applying its update function, i.e., an assignment of tokens to each place, defined by a marking expression (not present in Fig. 1). Ties (i.e., limit cases of synchronization among DET transitions with the same time-to-fire, e.g., occurring when they are enabled at the initial time) are solved by a random switch determined by probabilistic weights of transitions (not present in Fig. 1).

Fig. 1 shows the STPN of four parallel activities with uniformly distributed duration, modeled by the GEN transitions `act1`, `act2`, `act3`, and `act4`. The IMM transition `watchdog` fires as soon as activities represented by `act2`, `act3`, and `act4` have been completed while the activity represented by `act1` is still ongoing.

The SIRIO library [1] implements syntax and semantics of STPNs where GEN transitions have *exponential* CDF [56] (i.e., sums of products of exponentials and polynomials), including EXP, uniform, triangular, and Erlang CDFs.

2.2 Transient Evaluation by the Method of Stochastic State Classes

An SSC [57] comprises a marking, a joint support, and a PDF for vector $\langle \tau_{age}, \vec{\tau} \rangle$ encoding times-to-fire of the G enabled transitions and the absolute elapsed time (the “age” $\tau_{age} \in \mathbb{R}_{\geq 0}$). Given an SSC Σ , a succession relation provides the joint support and the joint PDF of $\langle \tau_{age}, \vec{\tau} \rangle$ conditioned on the firing of a transition γ .

Definition 1 (SSC). *An SSC is a tuple $\Sigma = \langle m, D_{\langle \tau_{age}, \vec{\tau} \rangle}, f_{\langle \tau_{age}, \vec{\tau} \rangle} \rangle$ where: $m \in \mathcal{M}$ is a marking; $f_{\langle \tau_{age}, \vec{\tau} \rangle}$ is the PDF (immediately after the previous firing) of the random vector $\langle \tau_{age}, \vec{\tau} \rangle$ including the age timer τ_{age} and the times-to-fire $\vec{\tau}$ of transitions enabled by m ; and, $D_{\langle \tau_{age}, \vec{\tau} \rangle} \subseteq \mathbb{R}^{G+1}$ is the support of $f_{\langle \tau_{age}, \vec{\tau} \rangle}$.*

Definition 2 (Succession relation). *$\Sigma' = \langle m', D', f'_{\langle \tau_{age}, \vec{\tau} \rangle} \rangle$ is the successor of $\Sigma = \langle m, D, f_{\langle \tau_{age}, \vec{\tau} \rangle} \rangle$ through transition γ with probability μ (i.e., $\Sigma \xrightarrow{\gamma, \mu} \Sigma'$), if, given that the marking is m and $\langle \tau_{age}, \vec{\tau} \rangle$ is distributed over D according to $f_{\langle \tau_{age}, \vec{\tau} \rangle}$, then the firing of γ has probability $\mu > 0$ in Σ and yields marking m' and vector of times to fire $\langle \tau'_{age}, \vec{\tau}' \rangle$ distributed over D' according to $f'_{\langle \tau_{age}, \vec{\tau} \rangle}$.*

From an initial SSC where the times-to-fire of the enabled transitions are independently distributed, the relation $\xrightarrow{\gamma, \mu}$ can be enumerated by computing firing probabilities and resulting joint supports D' and PDFs $f'_{\langle \tau_{age}, \vec{\tau} \rangle}$ of vector $\langle \tau_{age}, \vec{\tau} \rangle$: D' is a Difference Bounds Matrix (DBM), i.e., solution of a set of

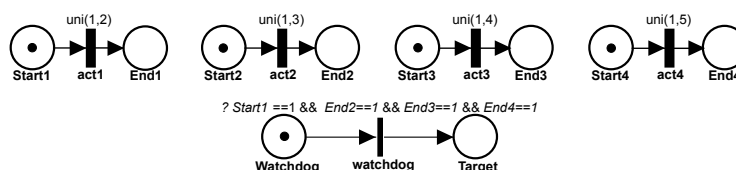


Fig. 1: STPN modeling four parallel overlapping activities

linear inequalities constraining the difference between two times-to-fire; for models with expolynomial GEN transitions, $f'_{\langle\tau_{age}, \vec{\tau}\rangle}$ takes piecewise analytical form (i.e., *multivariate expolynomial*) over a partition of D' in DBM sub-zones [16]. Enumeration of $\xrightarrow{\gamma, \mu}$ yields a transient tree: nodes are SSCs and edges are labeled with transitions and their firing probabilities [31]. Depending on the number of concurrent non-EXP transitions, after a large number of firings, the number of DBM-subzones may significantly increase, leading to a runtime explosion. For MRP models under the bounded regeneration restriction, the problem is largely mitigated by enumerating SSCs between any two regenerations [31], i.e., SSCs where all transitions are newly enabled or enabled by a DET time, and thus $f'_{\langle\tau_{age}, \vec{\tau}\rangle}$ takes the same analytical representation over the entire domain.

Given initial marking m_0 and PDF $f_{\langle\tau_{age}, \vec{\tau}\rangle}$ for $\langle\tau_{age}, \vec{\tau}\rangle$, the STPN semantics induces a probability space $\langle\Omega_{m_0}, \mathbb{F}_{\langle\tau_{age}, \vec{\tau}\rangle}, \mathbb{P}_{m_0, f_{\langle\tau_{age}, \vec{\tau}\rangle}}\rangle$: Ω_{m_0} is the set of feasible timed firing sequences and $\mathbb{P}_{m_0, f_{\langle\tau_{age}, \vec{\tau}\rangle}}$ is a probability measure over them [47].

An STPN identifies a Time Petri Net (TPN) [7,39] with same set of outcomes Ω_{m_0} . The state $\langle m, \langle\tau_{age}, \vec{\tau}\rangle \rangle$ of a TPN encodes marking $m \in \mathcal{M}$ and vector $\langle\tau_{age}, \vec{\tau}\rangle$ of the age timer and the times-to-fire of the enabled transitions. The state space is covered by State Classes (SCs), each SC $S = \langle m, D \rangle$ encoding marking m and joint support D for $\langle\tau_{age}, \vec{\tau}\rangle$. A reachability relation is defined between SCs: $S' = \langle m', D' \rangle$ is the successor of $S = \langle m, D \rangle$ via transition t if, from marking m and $\langle\tau_{age}, \vec{\tau}\rangle$ supported over D , t fires in S and yields marking m' and vector $\langle\tau_{age}, \vec{\tau}\rangle'$ supported over D' . From initial marking m_0 and domain D_0 for $\langle\tau_{age}, \vec{\tau}\rangle$, SC enumeration yields a State Class Graph (SCG) encoding the set of outcomes Ω_{m_0} , enabling correctness verification of the TPN.

In SSC $\Sigma = \langle m, D, f_{\langle\tau_{age}, \vec{\tau}\rangle} \rangle$, an enabled transition γ has null firing probability iff domain D conditioned on γ firing first has a non-null measure. Therefore, firings having null probability can be excluded from the SCG, which can then be used to determine reachability between SSCs, i.e., SSC $\Sigma' = \langle m', D', f'_{\langle\tau_{age}, \vec{\tau}\rangle} \rangle$ is reachable from SSC $\Sigma = \langle m, D, f_{\langle\tau_{age}, \vec{\tau}\rangle} \rangle$ iff SC $S' = \langle m', D' \rangle$ underlying Σ' is reachable from SC $S = \langle m, D \rangle$ underlying Σ . According to this, in the verification of time-bounded transient properties (e.g., probability that a marking condition is satisfied by time T), successor SSCs are enumerated iff target SSCs (i.e., those satisfying the property of interest) are reachable from them, which can be decided on the SCG, as just discussed. For very complex models for which the SCG enumeration is not viable, the marking graph could likely be enumerated (i.e., the graph encoding the reachability relation between markings), so as to avoid computation of the SSCs from which the target SSCs cannot be reached regardless of timing constraints. Alternatively, if the SCG not encoding the age variable can be enumerated, it could still be used to detect the SSCs from which the target SSCs are not reachable regardless of the elapsed time.

2.3 Monte Carlo Simulation and Importance Sampling

MC simulation performs n independent executions of an STPN, estimating the probability $p_\varphi(t)$ of marking condition φ at time t as the fraction of executions

that satisfy φ at time t . The state of an STPN is characterized by a Random Variable (RV) Y with support on the state space \mathcal{S} , where the samples y_i for $i \in \{1, 2, \dots, n\}$ describe a specific state. $p_\varphi(t)$ is the mean μ of a Bernoulli distributed RV $X = \Psi(Y)$, where $\Psi : \mathcal{S} \rightarrow \{0, 1\}$, whose independent samples x_i for $i \in \{1, 2, \dots, n\}$ are equal to either 1 or 0 depending on whether φ is satisfied at time t of the i -th execution or not, respectively. According to this, the mean μ and variance σ^2 of X can be estimated as the sample mean $\bar{X}_{sim} = \sum_{i=1}^n x_i/n$ and the variance $\bar{\sigma}_{sim}^2 = \bar{X}_{sim}(1 - \bar{X}_{sim})$, respectively. When using IS [33], samples are associated with a likelihood $L : \mathcal{S} \rightarrow \mathbb{R}_{\geq 0}$ to compensate for the change of PDF. Here, we estimate the mean μ of the reward with the sample mean $\bar{X}_{IS} = \sum_{i=1}^n L(y_i)\Psi(y_i)/n$ and the variance σ^2 with the sample variance [37]:

$$\tilde{\sigma}_{IS}^2 = \frac{1}{n-1} \sum_{i=1}^n \Psi^2(y_i)L^2(y_i) - \frac{n}{n-1} \bar{X}_{IS}^2 \quad (1)$$

By the central limit theorem, for large enough n , the distribution of $\sqrt{n}(\bar{X}_{sim} - \mu)/\sigma$ converges to the standard normal distribution, which also applies to \bar{X}_{IS} . Therefore, the CI for the target probability $p_\varphi(t)$ can be derived as:

$$\left[\bar{X}_{sim} - z_{\alpha/2} \cdot \frac{\tilde{\sigma}_{sim}}{\sqrt{n}}, \bar{X}_{sim} + z_{\alpha/2} \cdot \frac{\tilde{\sigma}_{sim}}{\sqrt{n}} \right], \quad (2)$$

where $z_{\alpha/2}$ corresponds to the $\alpha/2$ -quantile of the standard normal distribution.

3 Switch from Stochastic State Classes to Simulation

In this section, we provide an overview of our approach, resorting to an initial SSC expansion and simulation afterwards (Sec. 3.1); we explain how an SSC is conditioned on a transition firing to start a simulation offspring from it (Sec. 3.2); and, we describe how samples are created from a conditioned SSC (Sec. 3.3).

3.1 Approach Overview

We start with performing an analytical expansion with SSCs using a predefined depth d , meaning that we only enumerate SSCs: *i*) that can be reached at maximum after d transition firings, and *ii*) from which an SSC satisfying target property φ can be reached with positive probability (which can be decided on the underlying SCG—see Sec. 2.2). From each SSC Σ at distance d from the root, for each enabled transition γ of Σ such that a state satisfying φ can be reached from the successor SSC of Σ , we define a starting state for simulation offspring with pair $\langle \Sigma, \gamma \rangle$. Let the RV $Y_{\langle \Sigma, \gamma \rangle}$ with support on $\mathbb{R}_{\geq 0}^{G+1}$ denote the age τ_{age} and times-to-fire of the G enabled transitions for a simulation offspring (from a $(G+1)$ -dimensional SSC Σ) when γ fires first. For given model time t and property φ , let the RV $X_{\langle \Sigma, \gamma \rangle}$ with support on $\{0, 1\}$ denote the reward obtained when evaluating φ by performing a simulation run $\Psi_{\langle \Sigma, \gamma \rangle} : \mathbb{R}_{\geq 0}^{G+1} \times \mathcal{S} \rightarrow \{0, 1\}$ from

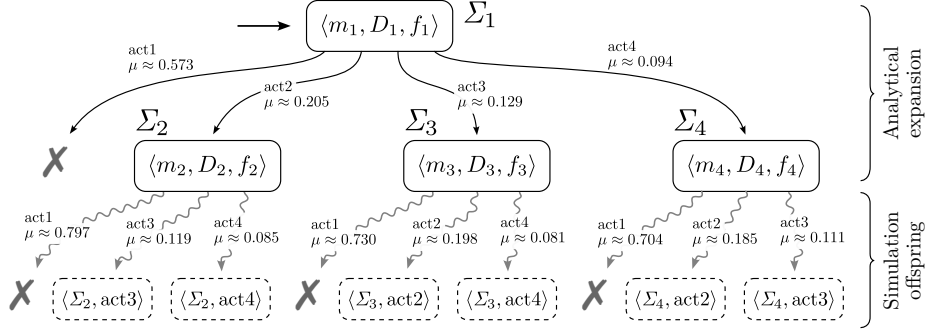


Fig. 2: Illustration of the approach with analytical expansion depth $d = 1$

pair $\langle \Sigma, \gamma \rangle$ until reaching time t . For simplicity, we omit the information of the simulation engine when referring to $\Psi_{\langle \Sigma, \gamma \rangle}$, so we write $X_{\langle \Sigma, \gamma \rangle} = \Psi_{\langle \Sigma, \gamma \rangle}(Y_{\langle \Sigma, \gamma \rangle})$.

Note that, other than belonging to the expolynomial class, no assumptions are made about the distributions of the RVs, nor on the presence of regeneration points. This makes our approach applicable to a general class of stochastic processes, including e.g. MRPs and some non-Markovian systems. For the model in Fig. 1 and expansion depth $d = 1$, Fig. 2 illustrates the procedure: after the firing of transition **act1**, any further analysis can be omitted, since the target condition (i.e., that the activity **act1** is still ongoing while **act2**, **act3**, and **act4** have been completed) can never be reached after this event has happened.

3.2 Conditioning Stochastic State Classes on Fired Transition

To define a starting state for a simulation offspring associated with pair $\langle \Sigma, \gamma \rangle$, the age variable τ_{age} and the times-to-fire of the enabled transitions are sampled from the joint PDF $f_{\langle \tau_{age}, \vec{\tau} \rangle}$ of Σ conditioned on transition γ firing first. To this end, the times-to-fire of EXP transitions can be handled independently of τ and the other times-to-fire, given that, due to the memoryless property, those RVs are independent of the other ones and, after a transition firing, each of them follows its respective EXP distribution with the same rate [15]. In detail, we only store the rates $\lambda_1, \dots, \lambda_n$ of the involved EXP distributions, which however can influence the evolution of the other times-to-fire, as discussed in the following.

Σ is conditioned on transition γ firing first by the following steps (if EXP transitions are not present, then steps 1, 2, and 3a are omitted and, in step 3b, variable x_{exp} is not present and thus eq. (8) does not need to be solved):

1. We calculate the aggregated EXP distribution with rate $\lambda_{agg} = \lambda_1 + \dots + \lambda_n$, being the rate of the firing time of any of these transitions (as the minimum of n EXP RVs with rates $\lambda_1, \dots, \lambda_n$ is an EXP RV with rate $\lambda_1 + \dots + \lambda_n$).
2. We add the aggregated EXP time-to-fire to the joint PDF:

$$f_{\tau'}(x_{age}, \vec{x}, x_{exp}) = f_{\langle \tau_{age}, \vec{\tau} \rangle}(x_{age}, \vec{x}) \cdot e^{-\lambda_{agg} x_{exp}} \quad (3)$$

where $\tau' = \langle \tau_{age}, \vec{\tau}, \tau_{exp} \rangle$ and D' is the domain of $f_{\tau'}$.

3. We distinguish whether the fired transition γ is EXP itself or not:
- (a) If yes, x_{exp} is at most the time-to-fire of each non-EXP transition, and it fires with probability μ_γ , yielding the conditioned joint PDF $f_{\tau''}$, with $\tau'' = \langle \tau'_{age}, \vec{\tau}', \tau'_{exp} \rangle$ and $I = \{i \mid i \neq age \wedge i \neq exp\}$:

$$\mu_\gamma = \frac{\lambda_\gamma}{\lambda_{exp}} \int_{\substack{\{(x_{age}, \vec{x}, x_{exp}) \in D' \\ \text{s.t. } x_{exp} \leq x_i \ \forall i \in I\}}} f_{\tau'}(x_{age}, \vec{x}, x_{exp}) dx_{age} d\vec{x} dx_{exp} \quad (4)$$

$$f_{\tau''}(x_{age}, \vec{x}, x_{exp}) = \frac{\mathbf{1}_{\substack{\{(x_{age}, \vec{x}, x_{exp}) \in D' \\ \text{s.t. } x_{exp} \leq x_i \ \forall i \in I\}}(x_{age}, \vec{x}, x_{exp})}{\mu_\gamma \cdot \frac{\lambda_{exp}}{\lambda_\gamma}} \cdot f_{\tau'}(x_{age}, \vec{x}, x_{exp}) \quad (5)$$

- (b) Otherwise (the fired transition γ is not EXP), then x_γ must be at most x_{exp} or the time-to-fire of every non-EXP transition. It fires with probability μ_γ , yielding $f_{\tau''}$ with $\tau'' = \langle \tau'_{age}, \vec{\tau}', \tau'_{exp} \rangle$ and $I = \{i \mid i \neq age \wedge i \neq \gamma\}$:

$$\mu_\gamma = \int_{\{(x_{age}, \vec{x}, x_{exp}) \in D' \mid x_\gamma \leq x_i \ \forall i \in I\}} f_{\tau'}(x_{age}, \vec{x}, x_{exp}) dx_{age} d\vec{x} dx_{exp} \quad (6)$$

$$f_{\tau''}(x_{age}, \vec{x}, x_{exp}) = \frac{\mathbf{1}_{\substack{\{(x_{age}, \vec{x}, x_{exp}) \in D' \\ \text{s.t. } x_\gamma \leq x_i \ \forall i \in I\}}(x_{age}, \vec{x}, x_{exp})}{\mu_\gamma} f_{\tau'}(x_{age}, \vec{x}, x_{exp}) \quad (7)$$

As EXP times-to-fire are not affected by transition firings, $f_{\tau''}$ can be marginalized with respect to x_{exp} , yielding $f_{\tau'''}$ with $\tau''' = \langle \tau''_{age}, \vec{\tau}'' \rangle$:

$$f_{\tau'''}(x_{age}, \vec{x}) = \int_0^\infty f_{\tau''}(x_{age}, \vec{x}, x_{exp}) dx_{exp} \quad (8)$$

Given the firing probability μ_γ of γ in SSC Σ , we compute weight $w_{\langle \Sigma, \gamma \rangle} = \rho(\Sigma) \cdot \mu_\gamma$ where $\rho(\Sigma)$ is the reaching probability of Σ , and $w_{\langle \Sigma, \gamma \rangle}$ comprises the probability of reaching the successor SSC of Σ through γ starting from Σ . This quantity is needed to compute the global reward X by its individual rewards $X_{\langle \Sigma, \gamma \rangle}$, obtained from simulation offspring with pair $\langle \Sigma, \gamma \rangle$ (see Sec. 4).

Besides the rates of EXP transitions, we store the values of DET transitions and times-to-fire of transitions with DET time difference to the time-to-fire of another transition. Due to space limits, we refer to [15,57] for evaluation of the firing probability μ_γ and conditioned joint PDF with DET transitions.

3.3 Sampling Methods

Given an SSC conditioned on a transition firing, times-to-fire of EXP transitions can be sampled individually, while inverse transform cannot be applied for their joint PDF $f_{\langle \tau_{age}, \vec{\tau} \rangle}$ with τ_{age} , which takes a piece-wise expolynomial representation over a domain partition in DBM sub-zones. Therefore, we exploit two sampling methods that only need to evaluate $f_{\langle \tau_{age}, \vec{\tau} \rangle}$ at certain points, namely the Metropolis-Hastings (MH) algorithm [30,42] and IS [33]. They operate differently (in particular, in contrast to IS, MH algorithm generates samples with the same likelihood) and thus yield different CI evaluations in Sec. 4. We provide here a short description of these methods—for further details see Appendix B.

Metropolis-Hastings Algorithm. Starting from an arbitrary point in the PDF domain, we iteratively sample a new point \vec{x}' from a proposal PDF based on the last point \vec{x}_t (e.g., normal PDF centered at \vec{x}_t), accepting \vec{x}' with probability $\min(\alpha, 1)$ where $\alpha = f(\vec{x}')/f(\vec{x}_t)$ (acceptance ratio). Assessed by measuring autocorrelation of samples with the Ljung-Box test [41], we perform undersampling to ensure a low correlation between consecutive simulation offspring.

Importance Sampling. We introduce a proposal PDF \tilde{f} with a known sampler, whose domain \tilde{D} contains the original domain D , such as

$$\tilde{f}(\vec{x}) = \prod_{i=1}^H \mathbf{1}_{[l_i, u_i]}(x_i) \begin{cases} \frac{1}{u_i - l_i} & \text{if } l_i \neq -\infty \wedge u_i \neq \infty \\ \lambda e^{-\lambda(x_i - l_i)} & \text{else if } u_i = \infty \\ \lambda e^{-\lambda(u_i - x_i)} & \text{else if } l_i = -\infty \end{cases}, \quad (9)$$

where l_i and u_i are the lower and upper bound, respectively, of the marginal domain of x_i with $i \in \{1, \dots, H\}$, where $H \leq G + 1$ is the number of non-EXP and non-DET transitions involved, and $\lambda \in \mathbb{R}^+$ is a parameter defined by the user. Note that λ has to be chosen carefully (e.g. neither too low nor too high) to avoid variance explosion [37]. Also note that, as τ_{age} is encoded as the opposite of the elapsed time in the calculus of SSCs, we consider the case that $l_i = -\infty$.

4 Collecting Results and Obtaining Confidence Intervals

In this section, we illustrate the derivation of CIs. We characterize the states that fulfill the target time-bounded transient property φ in three cases:

- If φ is satisfied by a state during simulation from pair $\langle \Sigma, \gamma \rangle$ (as described in Sec. 3), we estimate the mean $\mu_{\langle \Sigma, \gamma \rangle}$ of the reward with the sample mean

$$\bar{X}_{\langle \Sigma, \gamma \rangle} = \frac{1}{n_{\langle \Sigma, \gamma \rangle}} \cdot \sum_{i=1}^{n_{\langle \Sigma, \gamma \rangle}} L(y_{\langle \Sigma, \gamma \rangle, i}) \Psi(y_{\langle \Sigma, \gamma \rangle, i}) \quad (10)$$

using simulation offspring times $y_{\langle \Sigma, \gamma \rangle, i}$, $i \in \{1, \dots, n_{\langle \Sigma, \gamma \rangle}\}$, from $Y_{\langle \Sigma, \gamma \rangle}$. It converges, according to the central limit theorem, to a normal distribution:

$$\bar{X}_{\langle \Sigma, \gamma \rangle} \rightarrow \mathcal{N} \left(\mu_{\langle \Sigma, \gamma \rangle}, \frac{\sigma_{\langle \Sigma, \gamma \rangle}^2}{n_{\langle \Sigma, \gamma \rangle}} \right) \quad (11)$$

As described in Sec. 2.3, if samples have the same weight (e.g., $L(y_{\langle \Sigma, \gamma \rangle, i}) = 1$, which holds for the MH algorithm), we estimate the variance with $\tilde{\sigma}_{\langle \Sigma, \gamma \rangle}^2 = \bar{X}_{\langle \Sigma, \gamma \rangle} (1 - \bar{X}_{\langle \Sigma, \gamma \rangle})$. When incorporating weights of samples with IS, we estimate the variance by the sample variance:

$$\begin{aligned} \tilde{\sigma}_{\langle \Sigma, \gamma \rangle}^2 &= \frac{1}{n_{\langle \Sigma, \gamma \rangle} - 1} \sum_{i=1}^{n_{\langle \Sigma, \gamma \rangle}} \Psi_{\langle \Sigma, \gamma \rangle}^2(y_{\langle \Sigma, \gamma \rangle, i}) L_{\langle \Sigma, \gamma \rangle}^2(y_{\langle \Sigma, \gamma \rangle, i}) \\ &\quad - \frac{n_{\langle \Sigma, \gamma \rangle}}{n_{\langle \Sigma, \gamma \rangle} - 1} (\bar{X}_{\langle \Sigma, \gamma \rangle})^2 \end{aligned} \quad (12)$$

- If φ is satisfied by SSC Σ_{det} , then: if φ requires some property (marking condition) to be satisfied at time t , the weight is the reaching probability $\rho(\Sigma_{det})$ multiplied by the probability that Σ_{det} is the last SSC reached at t :

$$w_{\Sigma_{det}} = \rho(\Sigma_{det}) \int_{\{(x_{age}, \vec{x}) \in D \text{ s.t. } -x_{age} \leq t \wedge x_i - x_{age} > t \ \forall i\}} f_{\langle \tau_{age}, \vec{\tau} \rangle}(x_{age}, \vec{x}) dx_{age} d\vec{x} \quad (13)$$

Otherwise, if φ requires some property be satisfied within time t , then $w_{\Sigma_{det}}$ is derived as $\rho(\Sigma_{det})$ multiplied by the probability that Σ_{det} is reached within t :

$$w_{\Sigma_{det}} = \rho(\Sigma_{det}) \int_{\{(x_{age}, \vec{x}) \in D \text{ s.t. } -x_{age} \leq t\}} f_{\langle \tau_{age}, \vec{\tau} \rangle}(x_{age}, \vec{x}) dx_{age} d\vec{x} \quad (14)$$

- If an SSC satisfying φ is unreachable from an SSC (which can be decided using the SCG, see Sec. 2.2), SSC expansion is stopped, yielding reward zero.

Combining the results of the first two cases, we estimate the total reward by eq. (15), and then we can calculate the CI for the estimator by Theorem 1:

$$\bar{X}_{mixed} = \sum_{\langle \Sigma, \gamma \rangle} w_{\langle \Sigma, \gamma \rangle} \cdot \bar{X}_{\langle \Sigma, \gamma \rangle} + \sum_{\Sigma_{det}} w_{\Sigma_{det}} \quad (15)$$

Theorem 1 (Confidence Interval for composite analysis). *The $1 - \alpha$ CI of the mean μ for the estimator in eq. (15) can be calculated with*

$$[\bar{X}_{mixed} - z_{\alpha/2} \cdot \sigma_{mixed}, \bar{X}_{mixed} + z_{\alpha/2} \cdot \sigma_{mixed}],$$

where $z_{\alpha/2}$ corresponds to the $\alpha/2$ -quantile for the standard normal distribution $\mathcal{N}(0, 1)$ and σ_{mixed}^2 is defined as:

$$\sigma_{mixed}^2 = \sum_{\langle \Sigma, \gamma \rangle} \frac{w_{\langle \Sigma, \gamma \rangle}^2}{n_{\langle \Sigma, \gamma \rangle}} \cdot \sigma_{\langle \Sigma, \gamma \rangle}^2$$

Proof. The estimator in eq. (15) consists of the weighted sum of individual estimates for each combination of SSC and outgoing transition. As denoted in eq. (11), each individual sum converges to a normal distribution. The deterministic values $w_{\Sigma_{det}}$ can also be interpreted as $\mathcal{N}(w_{\Sigma_{det}}, 0)$. Furthermore, for two independent random variables $Y \sim \mathcal{N}(\mu_Y, \sigma_Y^2)$ and $Z \sim \mathcal{N}(\mu_Z, \sigma_Z^2)$, the sum $Y + Z$ is distributed according to $\mathcal{N}(\mu_Y + \mu_Z, \sigma_Y^2 + \sigma_Z^2)$. Besides, $\text{Var}(aY) = a^2 \text{Var}(Y)$ holds for the variance of a random variable Y with constant $a \in \mathbb{R}_{\geq 0}$. Using this information, we obtain that the estimator in eq. (15) converges to a normal distribution $\mathcal{N}(\mu, \sigma_{mixed}^2)$ with:

$$\bar{X}_{mixed} \rightarrow \mathcal{N} \left(\sum_{\langle \Sigma, \gamma \rangle} w_{\langle \Sigma, \gamma \rangle} \cdot \mu_{\langle \Sigma, \gamma \rangle} + \sum_{\Sigma_{det}} w_{\Sigma_{det}}, \sum_{\langle \Sigma, \gamma \rangle} \frac{w_{\langle \Sigma, \gamma \rangle}^2}{n_{\langle \Sigma, \gamma \rangle}} \cdot \sigma_{\langle \Sigma, \gamma \rangle}^2 \right)$$

The expression $(\bar{X}_{mixed} - \mu) / \sigma_{mixed}$ then converges to a standard normal distribution $\mathcal{N}(0, 1)$ for a sufficiently large sample size. Thus, we can rearrange the formula and calculate the CI as usual. \square

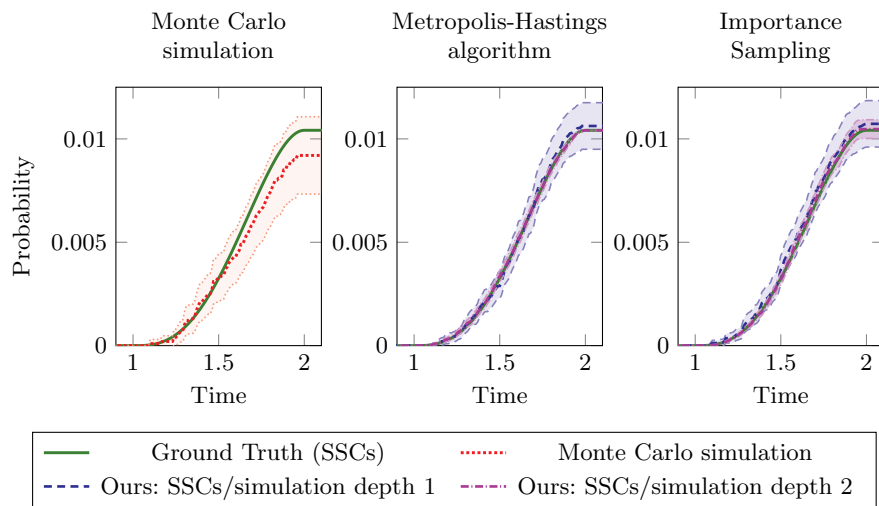


Fig. 3: Transient probabilities for four overlapping activities with 95% CIs

5 Experimental Evaluation

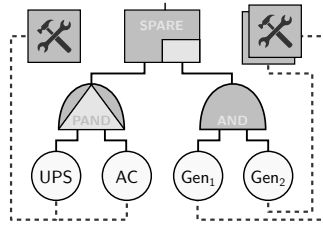
In this section, we evaluate the approach with the example of Fig. 1 (Sec. 5.1) and a Dynamic Fault Tree (DFT) case study (Sec. 5.2). A prototype implementation was developed using the Sirio library [1], which supports STPNs and SSCs, and enables experimentation on general stochastic processes—see Sections 2.1 and 3.1. Experiments were performed on an Apple M1 CPU with 16 GB RAM.

5.1 Four Overlapping Activities

The first scenario is the model with four parallel overlapping activities from Fig. 1, for which Fig. 2 illustrated the mixture of SSCs analysis and simulation offspring. Although this model can be fully analyzed analytically, we use it here to investigate the effects of different SSC expansion depths and the two sampling methods. We study the probability that the system fails up to some model time t , i.e. the PCTL-like property $P(F_{\leq t} \text{Target} = 1)$. Fig. 3 depicts the transient probabilities for this model when using different analysis techniques:

1. **MC simulation**: 10000 simulation runs \rightarrow 1085 ms analysis runtime;
2. **Ours: SSCs/simulation depth 1**: 500 simulation offspring per SSC/transition pair \rightarrow 14476 ms (MH algorithm)/702 ms (IS) runtime;
3. **Ours: SSCs/simulation depth 2**: 200 simulation offspring per SSC/transition pair \rightarrow 5290 ms (MH algorithm)/800 ms (IS) runtime;
4. **Ground Truth**: build complete SSC tree \rightarrow 809 ms analysis runtime.

As can be seen, regular MC simulation shows the widest CI and the largest deviation from the Ground Truth, while the two other methods successively narrow

Fig. 4: Repairable DFT⁴

```

1 toplevel "Target";
2 "Target" spare "PAND" "AND";
3 "PAND" pand "UPS" "AC";
4 "AND" and "Gen1" "Gen2";
5 "UPS" fail-uni(9.95,12) repair-exp(5);
6 "AC" fail-uni(18,20) repair-uni(0,0.5);
7 "Gen1" fail-exp(1 dorm-dir(∞) repair-uni(1,2);
8 "Gen2" fail-exp(2 dorm-dir(∞) repair-uni(2,4);
9 "R_PAND" rbox prio "UPS" "AC";
10 "R_GEN1" rbox prio "Gen1";
11 "R_GEN2" rbox prio "Gen2";

```

Code 1: DFT from Fig. 4 in Kepler syntax [11]

the width of the CIs. In the end, the second tested method performs in total $(3 \cdot 2) \cdot 500 = 3000$ simulation runs, while the third one does $(3 \cdot 2 \cdot 1) \cdot 200 = 1200$ simulation runs. Thus, both methods resulted in a higher accuracy while performing fewer simulation runs than crude MC simulation. When comparing the MH algorithm and IS for creating simulation offspring, we notice a high runtime difference between the two methods. This stems from the high undersampling step of 800 needed for MH according to the Ljung-Box test to obtain uncorrelated simulation offspring (see Appendix B). Furthermore, with SSC expansion depth $d = 2$, sampling with MH results in a zero-variance estimate for $t \geq 2$, while we observe non-zero variance when resorting to IS. The reason for this is that for MH we can estimate the variance with $\hat{\sigma}_{\langle \Sigma, \gamma \rangle}^2 = \bar{X}_{\langle \Sigma, \gamma \rangle} (1 - \bar{X}_{\langle \Sigma, \gamma \rangle})$, while for IS we resort to eq. (12). Since every simulation employed from depth $d = 2$ always reaches the target state, the corresponding mean equals 1. Thus, the estimator for MH returns variance zero, whereas we obtain for IS non-zero variance due to the different likelihood of the samples.

5.2 Repairable Dynamic Fault Tree

For a more complex example, we study a repairable DFT following the semantics of [43]. Our model uses the AND, PAND, and SPARE gates shown in Fig. 4 and code 1, as well as three repair boxes where the repair priority of the left one is first UPS, then AC.⁴ This models a highly reliable system powered by an unreliable grid, which has a UPS to remain operational during the recurrent blackouts. The UPS battery is replaced periodically: if during the replacement a blackout occurs, an emergency mechanism turns on two diesel generators. If both generators fail during the blackout, and before the UPS battery has been replaced, a system failure occurs. We measure the probability of system failure before 21 time units elapse, i.e. the transient PCTL-like property $P(F_{\leq 21} \text{Target} = 1)$.

This DFT has two failure modes, with the AND modeling a race condition of EXP random variables and uniformly distributed revert transitions—*repairs*—

⁴ The children of a SPARE in [43] are Basic Elements (BEs) or spare BEs. We extend this for cold SPAREs [32], with an inactive *spare subtree*—the right AND gate—that cannot fail while the *primary subtree*—the left PAND gate—is operational. Repairs of the primary subtree reset the spare subtree state (cf. spare BE semantics [11,43]).

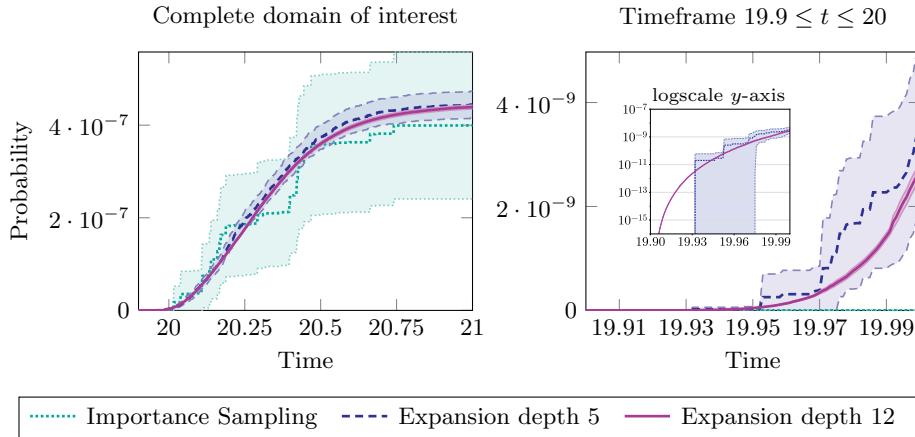


Fig. 5: Transient probabilities for repairable DFT example with 95% CIs

analyzable, e.g., via MC or IS. In contrast, PAND failures require UPS to fail before AC, and are reverted when AC is repaired. The failure and repair distributions of the BEs make PAND failures a rare event that rules out MC analysis. Time-agnostic ISPLIT approaches such as [11] are equally impractical. IS could work, but requires non-trivial proposal failure PDFs of UPS and AC, which result in more frequent failures in the proper order. Instead, expansions with SSCs can cover the PAND analytically, and afterwards, one can resort to MC or IS to study AND failures. We experiment with these different approaches as follows:

1. **Importance Sampling:** We set up a mixture of PDFs for the failure of UPS and AC, to increase the probability of their ordered failure before repair:

$$\text{UPS} \sim \begin{cases} \text{Unif}(9.95, 10) & \text{with } 50\%, \\ \text{Unif}(10, 12) & \text{with } 50\%; \end{cases} \quad \text{AC} \sim \begin{cases} \text{Unif}(18, 19.9) & \text{with } 50\%, \\ \text{Unif}(19.9, 20) & \text{with } 50\%. \end{cases}$$

We perform 50000 simulation runs and observe a runtime of 44.7 s.

2. **Ours: SSC/simulation depth 5:** We perform 10000 simulation offspring per SSCs/transition pair, observing a runtime of 7.8 s.
3. **Ours: SSC/simulation depth 12:** As above, with 41.0 s of runtime.

In our combined SSC/simulation approach we use only IS for creating simulation offspring, as the need for a high undersampling step renders MH impractical. SSC expansions of depth ≥ 5 suffice to analytically cover the PAND gate failure—i.e. when the second UPS failure occurs before the AC failure—resulting in a useful mixture of SSCs and simulation. However, too-high expansion depths beyond 12 lead to a runtime explosion for SSC analysis, mainly due to the complexity stemming from splitting the analytical representation into subdomains.

Fig. 5 shows how our mixed SSC/simulation analysis results in a higher accuracy than IS. Moreover, applying IS to this example required non-trivial

human insight, and the beneficial (or detrimental) effect of the proposed PDFs is not immediately clear, as opposed to the choice of the SSC expansion depth. In that last respect, expanding up to depth 12 results in a (partial) analytical coverage of the target states, which is why the mixed SSC/simulation approach can detect probabilities below 10^{-14} near $t = 19.9$ —see the right plot in Fig. 5.

6 Conclusion

In this paper, we presented an approach to compute transient probabilities by first performing an analytical expansion with SSCs and then resorting to simulation. We presented two different solutions to create simulation offspring, namely the MH algorithm and the IS method, where the latter seems to be preferable due to the fact that it does not require undersampling. For both methods, we demonstrated how to derive confidence intervals. Our prototype was evaluated with two examples: (a) four overlapping parallel activities and (b) a repairable DFT, where the latter demonstrated how this composite analysis method can outperform classic RES techniques such as IS and ISPLIT.

The main drawback of the method for the applicability in RES is that it requires the critical event (that makes standard simulation impractical) to occur near the root of the state space. We see two ways to overcome this limitation. First, one could introduce multilevel switching from simulation to SSCs, similarly to ISPLIT, whenever a critical region is encountered. The challenging part is to detect when such a region occurs. Secondly—for specific model classes—we can exploit regenerations and run our approach for each regenerative epoch.

Furthermore, sensitivity studies would help to quantify the effect of the number of samples on the tradeoff between accuracy and time gain, e.g. for the example in Sec. 5.2. In this context, one challenge is to design more robust methods for deriving CIs. When dealing with a low probability or a small sample size, the target might never hit and we falsely assume a zero-variance with the variance estimators, e.g. $\bar{\sigma}_{sim}^2 = \bar{X}_{sim}(1 - \bar{X}_{sim})$ when using the MH algorithm to create simulation offspring. Analyses via standard MC simulation can use the Wilson score interval in such situations, as it provides better CI coverage [58]—we envision that similar techniques might be applicable to the combined SSCs/simulation approach as well.

Acknowledgments. We thank Pedro R. D’Argenio for the fruitful discussion that helped us with the derivation of Confidence Intervals. This work was partially funded by DFG grant 389792660 as part of TRR 248 – CPEC, the European Union under the INTERREG North Sea project *STORM-SAFE* of the European Regional Development Fund, the NRRP “Telecommunications of the Future” (PE00000001, *RESTART*), MSCA grant 101067199 (*ProSVED*), and the NextGenerationEU projects P2022A492B (*ADVENTURE*) and D53D230084-00006 (*SMARTITUDE*) under the MUR PRIN 2022 PNRR.

Data Availability Statement. A reproduction package for our experiments (i.e. the artifact of this paper) is available at [10.6084/m9.figshare.25665198](https://doi.org/10.6084/m9.figshare.25665198).

A Stochastic Time Petri Net of Dynamic Fault Tree

This section describes the STPN crafted for the repairable DFT example analyzed in Sec. 5.2, which is illustrated in Fig. 6. The initial marking of the STPN is $U_{ps} = 1, A_c = 1$ with enabled transitions u_{ps} and a_c , which characterize the failure times of the battery and the power system, respectively. Since both components share the same repair box, we need to implement a logic that ensures the mutual exclusion of the repairs. This is done using the transitions $u_{ps}Race$ and a_cRace , which marks the beginning of a repair process by adding a token to $U_{ps}Rep$ and A_cRep , respectively. Both $u_{ps}Race$ and a_cRace can only fire when there is no repair process ongoing (which occurs when places A_cRep and $U_{ps}Rep$ are empty, respectively). The repair itself is modeled by transitions $u_{ps}Rep$ and a_cRep , which removes the token from the place representing the corresponding failure ($U_{ps}Failed$ and $A_cFailed$, respectively), ending the repair process (represented by the firing of transitions $u_{ps}Rep$ and a_cRep , respectively), and updating the failure conditions of the PAND gate (modeled by places $U_{ps}First$ and $PandFailed$). Transition $checkU_{ps}$ fires when the power system has failed, but not the battery, which ensures the failure order of the PAND gate. The activation of both diesel generators is represented by the firing of $checkA_c$, which adds a token to $Gen1$ and $Gen2$. The repair of the PAND is modeled by transition $CheckPandRepair$, which fires after a failure of the PAND gate as soon as the battery is repaired, and switches off both diesel generators (by removing tokens from places $Gen1$, $Gen2$, $Gen1Failed$, and $Gen2Failed$). Similarly to the power system and the battery, the failure of diesel generators is modeled by transitions $gen1$ and $gen2$, respectively. Since both diesel generators have an individual repair box, no synchronization is necessary, and thus transitions $gen1Rep$ and $gen2Rep$ suffice. Finally, the transition $watchdog$ keeps track of the failure condition that both diesel generators fail and thus finally the SPARE gate, and adds a token to place $Target$ modeling a system failure.

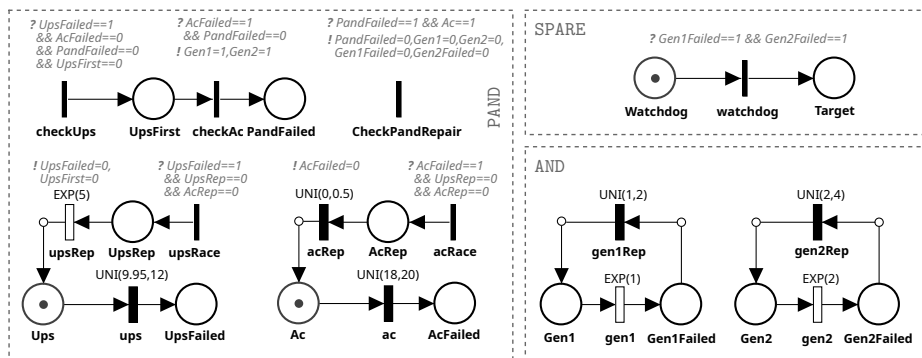


Fig. 6: STPN of the DFT shown in Fig. 4.

B Implementation Details of Sampling Methods

We provide implementation details and parameters used for the sampling methods for creating simulation offspring from SSCs.

For the MH algorithm, we begin with an arbitrary starting point inside the domain D of the SSC Σ . We obtain this point by uniform sampling from the multidimensional rectangle $\prod_{i=1}^H [l_i, u_i]$, where l_i and u_i are the minimum and maximum possible value of a variable, and checking if the obtained point lies inside D . When we are dealing with an infinite domain, we cap the lower and upper bound to a predefined value (however, this is not relevant here, as this case does not happen in the example presented in Fig. 1). In each step, we predict a new candidate x' with the help of a proposal PDF $g(x | y)$. We can calculate the acceptance ratio based on the evaluated PDF of the new candidate x' and the old point x_t . The acceptance ratio α is used to determine if the new point will be accepted or not. In our implementation, we use for $g(x | y)$ a separate normal distribution for each dimension that is centered around y with variance σ . To determine σ , we start with $\sigma = 1$ and perform a binary search-like warm-up procedure to ensure that σ is configured in a way such that the acceptance ratio lies on average between 0.2 and 0.3, which is compliant with the regular rule-of-thumb acceptance ratio of ≈ 0.234 [22]. In detail, we perform 100 rounds, where in each round we perform 100 MH steps and calculate the mean acceptance ratio. Depending on whether the acceptance ratio lies below 0.2 or above 0.3, we divide or multiply σ by 1.25 or leave σ unchanged. Furthermore, we determine an undersampling step for the obtained samples to ensure that the obtained samples are uncorrelated. We start with an undersampling step of 100, assess the autocorrelation with the multivariate Ljung-Box test [41], and increase the undersampling step incrementally by 100. In detail, we resorted to the Microsoft WPA library for R⁵, using 10^5 samples for each simulation start point when using an analytical expansion depth of $d = 1$ in the example of four overlapping activities shown in Fig. 1. Results indicate that an undersampling step of 800 is necessary to obtain uncorrelated samples.

For IS, as the variables of the proposal density in eq. (9) are stochastically independent, we handle each variable individually. Thereby, we calculate the likelihood for each variable by comparing the marginal densities of the proposal density and the true density and multiply these values to obtain the global likelihood. We reject samples that are only part of the proposal domain and not the original one to obtain only samples with non-zero likelihood. This makes it necessary to scale the likelihood of each sample afterwards by the probability that a sampled point from the proposal PDF \tilde{f} lies in the original domain D , which can be calculated with $\int_{\vec{x} \in D} \tilde{f}(\vec{x}) d\vec{x}$. We resorted to $\lambda = 1$, as the repairable DFT example in Fig. 4 deals with EXP transitions with rate 1 or 2.

⁵ See function documentation at: <https://microsoft.github.io/wpa/reference/LjungBox.html>

References

1. Sirio source code on GitHub, <https://github.com/oris-tool/sirio>, [Online; accessed 24th June 2024]
2. Agha, G., Palmkog, K.: A survey of statistical model checking. *ACM Trans. Model. Comput. Simul.* **28**(1), 6:1–6:39 (2018). <https://doi.org/10.1145/3158668>
3. Amparore, E.G., Donatelli, S.: A component-based solution for reducible markov regenerative processes. *Performance Evaluation* **70**(6), 400–422 (2013)
4. Andriushchenko, R., Bork, A., Budde, C.E., Češka, M., Grover, K., Hahn, E.M., Hartmanns, A., Israelsen, B., Jansen, N., Jeppson, J., Junges, S., Köhl, M.A., Könighofer, B., Křetínský, J., Meggendorfer, T., Parker, D., Pranger, S., Quatmann, T., Ruijters, E., Taylor, L., Volk, M., Weininger, M., Zhang, Z.: Tools at the frontiers of quantitative verification: QComp 2023 competition report. In: TACAS. vol. to appear (2024)
5. Baier, C., Katoen, J.P.: *Principles of Model Checking*. MIT Press (2008)
6. van der Berg, F., van de Pol, J.: Concurrent chaining hash maps for software model checking. In: FMCAD. pp. 46–54. IEEE (2019). <https://doi.org/10.23919/FMCAD.2019.8894279>
7. Berthomieu, B., Diaz, M.: Modeling and verification of time dependent systems using time petri nets. *IEEE transactions on software engineering* **17**(3), 259 (1991)
8. Biagi, M., Carnevali, L., Paolieri, M., Vicario, E.: Performability evaluation of the ERTMS/ETCS – Level 3. *Transportation Research Part C: Emerging Technologies* **82**, 314–336 (2017). <https://doi.org/10.1016/j.trc.2017.07.002>
9. de Boer, P., Kroese, D.P., Mannor, S., Rubinstein, R.Y.: A tutorial on the cross-entropy method. *Ann. Oper. Res.* **134**(1), 19–67 (2005). <https://doi.org/10.1007/S10479-005-5724-Z>
10. Budde, C.E., D’Argenio, P.R., Hartmanns, A., Sedwards, S.: An efficient statistical model checker for nondeterminism and rare events. *International Journal on Software Tools for Technology Transfer* **23**, 759–780 (2020). <https://doi.org/10.1007/s10009-020-00563-2>
11. Budde, C.E., D’Argenio, P.R., Monti, R.E., Stoelinga, M.: Analysis of non-Markovian repairable fault trees through rare event simulation. *International Journal on Software Tools for Technology Transfer* **24**(5), 821–841 (2022). <https://doi.org/10.1007/s10009-022-00675-x>
12. Buijsrogge, A., de Boer, P., Scheinhardt, W.R.W.: Importance sampling for Markovian tandem queues using subsolutions: exploring the possibilities. *Simul.* **97**(12) (2021). <https://doi.org/10.1177/00375497211041351>
13. Carnevali, L., Ciani, L., Fantechi, A., Gori, G., Papini, M.: An efficient library for Reliability Block Diagram evaluation. *Applied Sciences* **11**(9) (2021). <https://doi.org/10.3390/app11094026>
14. Carnevali, L., German, R., Santoni, F., Vicario, E.: Compositional Analysis of Hierarchical UML Statecharts. *IEEE Transactions on Software Engineering* **48**(12), 4762–4788 (2022). <https://doi.org/10.1109/TSE.2021.3125720>
15. Carnevali, L., Grassi, L., Vicario, E.: State-density functions over dbm domains in the analysis of non-markovian models. *IEEE Transactions on Software Engineering* **35**(2), 178–194 (2008)
16. Carnevali, L., Grassi, L., Vicario, E.: State-Density Functions over DBM Domains in the Analysis of Non-Markovian Models. *IEEE Transactions on Software Engineering* **35**(2), 178–194 (2009). <https://doi.org/10.1109/TSE.2008.101>

17. Chatterjee, K., Henzinger, T.A.: Value Iteration, LNCS, vol. 5000, pp. 107–138. Springer (2008). https://doi.org/10.1007/978-3-540-69850-0_7
18. Choi, H., Kulkarni, V.G., Trivedi, K.S.: Markov regenerative stochastic petri nets. *Performance evaluation* **20**(1-3), 337–357 (1994)
19. Ciardo, G., German, R., Lindemann, C.: A characterization of the stochastic process underlying a stochastic Petri net. *IEEE Transactions on software engineering* **20**(7), 506–515 (1994)
20. Dongliang, Z., Kaiwen, Z., Chaofan, Z.: Reliability modeling and analysis of reactor protection system based on FPGA. *Nuclear Power Engineering* **42**(5), 173–177 (2021). <https://doi.org/10.13832/j.jnpe.2021.05.0173>
21. Forejt, V., Kwiatkowska, M.Z., Norman, G., Parker, D.: Automated verification techniques for probabilistic systems. In: SFM. LNCS, vol. 6659, pp. 53–113. Springer (2011). https://doi.org/10.1007/978-3-642-21455-4_3
22. Gelman, A., Gilks, W.R., Roberts, G.O.: Weak convergence and optimal scaling of random walk Metropolis algorithms. *The Annals of Applied Probability* **7**(1), 110–120 (1997). <https://doi.org/10.1214/aoap/1034625254>
23. German, R., Telek, M.: Formal relation of Markov renewal theory and supplementary variables in the analysis of stochastic Petri nets. In: Proceedings 8th International Workshop on Petri Nets and Performance Models (Cat. No.PR00331). pp. 64–73 (1999). <https://doi.org/10.1109/PNPM.1999.796537>
24. German, R., Lindemann, C.: Analysis of stochastic Petri nets by the method of supplementary variables. *Performance Evaluation* **20**(1), 317–335 (1994). [https://doi.org/10.1016/0166-5316\(94\)90020-5](https://doi.org/10.1016/0166-5316(94)90020-5)
25. German, R., Lindemann, C.: Analysis of stochastic petri nets by the method of supplementary variables. *Performance evaluation* **20**(1-3), 317–335 (1994)
26. German, R., Logothetis, D., Trivedi, K.S.: Transient analysis of markov regenerative stochastic petri nets: A comparison of approaches. In: Proceedings 6th International Workshop on Petri Nets and Performance Models. pp. 103–112. IEEE (1995)
27. Grassmann, W.: Transient solutions in Markovian queues: An algorithm for finding them and determining their waiting-time distributions. *European Journal of Operational Research* **1**(6), 396–402 (1977). [https://doi.org/10.1016/0377-2217\(77\)90049-2](https://doi.org/10.1016/0377-2217(77)90049-2)
28. Hahn, E.M., Hartmanns, A., Hensel, C., Klauck, M., Klein, J., Kretínský, J., Parker, D., Quatmann, T., Ruijters, E., Steinmetz, M.: The 2019 Comparison of Tools for the Analysis of Quantitative Formal Models - (QComp 2019 Competition Report). In: TACAS. LNCS, vol. 11429, pp. 69–92. Springer (2019). https://doi.org/10.1007/978-3-030-17502-3_5
29. Hartmanns, A.: On the analysis of stochastic timed systems. Ph.D. thesis, Saarland University (2015), <http://scidok.sulb.uni-saarland.de/volltexte/2015/6054/>
30. Hastings, W.K.: Monte Carlo Sampling Methods Using Markov Chains and Their Applications. *Biometrika* **57**(1), 97–109 (1970), <http://www.jstor.org/stable/2334940>
31. Horváth, A., Paolieri, M., Ridi, L., Vicario, E.: Transient analysis of non-Markovian models using stochastic state classes. *Performance Evaluation* **69**(7), 315–335 (2012). <https://doi.org/10.1016/j.peva.2011.11.002>
32. Junges, S., Katoen, J., Stoelinga, M., Volk, M.: One net fits all - A unifying semantics of dynamic fault trees using GSPNs. In: PETRI NETS. LNCS, vol. 10877, pp. 272–293. Springer (2018). https://doi.org/10.1007/978-3-319-91268-4_14

33. Kloek, T., Kloek, T., Van Dijk, H.: Bayesian estimates of equation system parameters: An application of integration by monte carlo. *Econometrica* **46**, 1–19 (02 1978). <https://doi.org/10.2307/1913641>
34. Kulkarni, V.G.: Modeling and analysis of stochastic systems. Chapman and Hall/CRC (2016)
35. Larsen, K.G., Legay, A.: Statistical model checking: Past, present, and future. In: ISoLA. LNCS, vol. 9952, pp. 3–15. Springer (2016). https://doi.org/10.1007/978-3-319-47166-2_1
36. L’Ecuyer, P., Le Gland, F., Lezaud, P., Tuffin, B.: Splitting Techniques, chap. 3, pp. 39–61. In: Rubino and Tuffin [54] (2009). <https://doi.org/10.1002/9780470745403.ch3>
37. L’Ecuyer, P., Mandjes, M., Tuffin, B.: Importance Sampling in Rare Event Simulation, chap. 2, pp. 17–38. In: Rubino and Tuffin [54] (2009). <https://doi.org/10.1002/9780470745403.ch2>
38. Lee, J., Mitici, M.: Predictive aircraft maintenance: Modeling and analysis using stochastic Petri nets. In: ESREL. pp. 146–153 (2021). https://doi.org/10.3850/978-981-18-2016-8_050-cd
39. Lime, D., Roux, O.H.: Expressiveness and analysis of scheduling extended time petri nets. *IFAC Proceedings Volumes* **36**(13), 189–197 (2003)
40. Lindemann, C., Thümmler, A.: Transient analysis of deterministic and stochastic petri nets with concurrent deterministic transitions. *Performance Evaluation* **36**, 35–54 (1999)
41. Ljung, G.M., Box, G.E.P.: On a measure of lack of fit in time series models. *Biometrika* **65**(2), 297–303 (1978), <http://www.jstor.org/stable/2335207>
42. Metropolis, N., Rosenbluth, A.W., Rosenbluth, M.N., Teller, A.H., Teller, E.: Equation of state calculations by fast computing machines. *The journal of chemical physics* **21**(6), 1087–1092 (1953)
43. Monti, R.E., Budde, C.E., D’Argenio, P.R.: A compositional semantics for repairable fault trees with general distributions. In: LPAR. EPiC, vol. 73, pp. 354–372. EasyChair (2020). <https://doi.org/10.29007/P16V>
44. Neuts, M.F.: Matrix-geometric Solutions in Stochastic Models: An Algorithmic Approach. Baltimore: Johns Hopkins University Press (1981)
45. O’Connor, P.D.T., Kleyner, A.: Practical Reliability Engineering. John Wiley & Sons, Ltd (2011). <https://doi.org/10.1002/9781119961260>
46. Paolieri, M., Biagi, M., Carnevali, L., Vicario, E.: The ORIS Tool: Quantitative Evaluation of Non-Markovian Systems. *IEEE Trans. Software Eng.* **47**(6), 1211–1225 (2021). <https://doi.org/10.1109/TSE.2019.2917202>
47. Paolieri, M., Horváth, A., Vicario, E.: Probabilistic model checking of regenerative concurrent systems. *IEEE Transactions on Software Engineering* **42**(2), 153–169 (2015)
48. Parri, J., Sampietro, S., Vicario, E.: Faultflow: a tool supporting an mde approach for timed failure logic analysis. In: 2021 17th European Dependable Computing Conference (EDCC). pp. 25–32 (2021). <https://doi.org/10.1109/EDCC53658.2021.00011>
49. Reliability and maintainability symposium (2024), <https://rams.org>
50. Reibman, A., Trivedi, K.: Numerical transient analysis of Markov models. *Computers & Operations Research* **15**(1), 19–36 (1988). [https://doi.org/10.1016/0305-0548\(88\)90026-3](https://doi.org/10.1016/0305-0548(88)90026-3)
51. Reijsbergen, D., de Boer, P., Scheinhardt, W.R.W., Juneja, S.: Path-ZVA: General, efficient, and automated importance sampling for highly reliable Marko-

- vian systems. *ACM Trans. Model. Comput. Simul.* **28**(3), 22:1–22:25 (2018). <https://doi.org/10.1145/3161569>
52. Robert L., J.: Analysis of phase-type stochastic Petri nets with discrete and continuous timing. Tech. rep. (2000), <https://ntrs.nasa.gov/citations/20000120040>
 53. Rubino, G., Tuffin, B.: Introduction to Rare Event Simulation, chap. 1, pp. 1–13. In: Rubino and Tuffin [54] (2009). <https://doi.org/10.1002/9780470745403.ch1>
 54. Rubino, G., Tuffin, B. (eds.): Rare Event Simulation Using Monte Carlo Methods. Wiley (2009). <https://doi.org/10.1002/9780470745403>
 55. Telek, M., Horváth, A.: Transient analysis of age-mrspns by the method of supplementary variables. *Performance Evaluation* **45**(4), 205–221 (2001)
 56. Trivedi, K.S., Sahner, R.: Sharpe at the age of twenty two. *ACM SIGMETRICS Performance Evaluation Review* **36**(4), 52–57 (2009)
 57. Vicario, E., Sassoli, L., Carnevali, L.: Using Stochastic State Classes in Quantitative Evaluation of Dense-Time Reactive Systems. *IEEE Transactions on Software Engineering* **35**(5), 703–719 (2009). <https://doi.org/10.1109/TSE.2009.36>
 58. Wilson, E.B.: Probable inference, the law of succession, and statistical inference. *Journal of the American Statistical Association* **22**(158), 209–212 (1927). <https://doi.org/10.1080/01621459.1927.10502953>
 59. Younes, H.L.S., Simmons, R.G.: Probabilistic verification of discrete event systems using acceptance sampling. In: CAV. LNCS, vol. 2404, pp. 223–235. Springer (2002). https://doi.org/10.1007/3-540-45657-0_17
 60. Younes, H.L.S.: Verification and planning for stochastic processes with asynchronous events. Ph.D. thesis, Carnegie Mellon University (2005)
 61. Zimmermann, A.: Modeling and evaluation of stochastic petri nets with timenet 4.1. In: 6th International ICST Conference on Performance Evaluation Methodologies and Tools. pp. 54–63. IEEE (2012)
 62. Zuliani, P., Baier, C., Clarke, E.M.: Rare-event verification for stochastic hybrid systems. In: HSCC. pp. 217–226. ACM (2012). <https://doi.org/10.1145/2185632.2185665>